

Numerical simulation of tridimensional electromagnetic shaping of liquid metals

Michel Pierre, Jean R. Roche

► **To cite this version:**

Michel Pierre, Jean R. Roche. Numerical simulation of tridimensional electromagnetic shaping of liquid metals. [Research Report] RR-1687, INRIA. 1992, pp.18. inria-00076911

HAL Id: inria-00076911

<https://hal.inria.fr/inria-00076911>

Submitted on 29 May 2006

HAL is a multi-disciplinary open access archive for the deposit and dissemination of scientific research documents, whether they are published or not. The documents may come from teaching and research institutions in France or abroad, or from public or private research centers.

L'archive ouverte pluridisciplinaire **HAL**, est destinée au dépôt et à la diffusion de documents scientifiques de niveau recherche, publiés ou non, émanant des établissements d'enseignement et de recherche français ou étrangers, des laboratoires publics ou privés.

INRIA

UNITÉ DE RECHERCHE
INRIA-LORRAINE

Institut National
de Recherche
en Informatique
et en Automatique

Domaine de Voluceau
Rocquencourt
B.P. 105
78153 Le Chesnay Cedex
France
Tél.: (1) 39 63 55 11

Rapports de Recherche

1992



ème
anniversaire

N° 1687

Programme 6
Calcul Scientifique, Modélisation et
Logiciels numériques

NUMERICAL SIMULATION OF TRIDIMENSIONAL ELECTROMAGNETIC SHAPING OF LIQUID METALS

Michel PIERRE
Jean R. ROCHE

Mai 1992



★ R R - 1 6 8 7 ★

Numerical Simulation of Tridimensional Electromagnetic Shaping of Liquid Metals

Michel **PIERRE** and Jean R. **ROCHE**
Université de Nancy I
Département de Mathématiques, BP 239
URA-CNRS 750, Projet NUMATH INRIA Lorraine
54506 VANDOEUVRE LES NANCY Cédex, FRANCE

Abstract : We describe a numerical method to compute free surfaces in electromagnetic shaping and levitation of liquid metals. We use an energetic variational formulation based on the total energy and we apply optimization techniques to compute a critical point. The surfaces are represented by piecewise linear finite elements.

Keywords: Shape optimization, levitation, Electromagnetic shaping, Boundary integral representation.

Simulation Numérique Tridimensionnelle en Formage Electromagnétique de métaux liquides.

Résumé : On décrit ici une méthode numérique pour le calcul de surfaces libres dans des problèmes de formage électromagnétique et de lévitation d'un métal liquide. Nous utilisons des techniques d'optimisation liées à la minimisation de la fonctionnelle d'énergie totale. La surface libre est représentée par des éléments finis linéaires par morceaux.

Numerical Simulation of Tridimensional Electromagnetic Shaping of Liquid Metals

Michel **PIERRE** and Jean R. **ROCHE**
 Université de Nancy I
 Département de Mathématiques, BP 239
 URA-CNRS 750, Projet NUMATH INRIA Lorraine
 54506 VANDOEUVRE LES NANCY Cédex, FRANCE

1. Introduction.

Our goal is to develop numerical method to compute free surfaces in electromagnetic shaping and levitation of liquid metals. We introduce quasi-Newton optimization techniques in an energetic variational formulation framework.

In the two-dimensional case a numerical simulation has been developed (see [20], [25], [5], [4], [10], [2], [17], [16]). The physical model concerns the case of a vertical column of liquid metal falling down in an electromagnetic field created by vertical conductors. We assume the frequency of the imposed current in very high so that the magnetic field does not penetrate into the metal and the electromagnetic forces are reduced to the magnetic pressure acting on the interface.

The same model in the tridimensional case represents a bubble of liquid metal levitating in an electromagnetic field. We want to compute the shape of the bubble (see [3], [11], [12], [13], [14]).

We denote by ω the exterior in \mathbb{R}^3 of the domain filled by the liquid metal and by Γ its boundary (here a surface).

The surface Γ is characterized by the following equilibrium equations :

$$(1.1) \quad \nabla \wedge B = \mu_0 j_0 \quad \text{in } \omega$$

$$(1.2) \quad \nabla \cdot B = 0 \quad \text{in } \omega$$

$$(1.3) \quad B \cdot n = 0 \quad \text{on } \Gamma = \partial\omega$$

$$(1.4) \quad \frac{\|B\|^2}{2\mu_0} + \sigma \mathcal{C} + \rho g z = \text{constant} = P \quad \text{on } \Gamma$$

where j_0 in the current density, B the magnetic field, μ_0 the magnetic permeability, q the density of the charge, g the gravitational acceleration, z the height, \mathcal{C} the mean curvature of Γ , σ the surface tension and n the unit normal vector directed towards ω . The constant P is an unknown of the problem. We denote by $\Omega = {}^c \omega$ the complement of ω .

The total energy of the system is given by (see [3], [28], [27], [9])

$$(1.5) \quad E(\Omega) = \frac{-1}{2\mu_0} \int_{\omega} \|B\|^2 dx + \sigma \int_{\Gamma} d\gamma + \int_{\Omega} \rho g z dx$$

where B is solution of (1.1) - (1.3). With some usual hypotheses, a critical point of $E(\Omega)$ under the constraint that $\text{meas}(\Omega)$ be given, satisfies the nonlinear equilibrium relation (1.4) which characterizes the boundary Γ .

A quasi-Newton optimization method is used here to compute a critical point of the total energy $\Omega \rightarrow E(\Omega)$. This means that one must compute the gradient of E with respect to Ω at each iteration. The main part of the gradient computation is solving the exterior problem (1.1) - (1.3) for each intermediate domain Ω_k . For this we introduce a boundary integral representation on the surface $\Gamma_k = \partial \Omega_k$. This is quite convenient here since the computation of the gradient of E requires only the values of the magnetic field on the surface Γ_k . The computation is done by using a piecewise linear approximation of Ω . The energy (1.5) is replaced by a corresponding discretized energy. Details are given in section 4. The derivatives with respect to Ω of the various terms in $E(\Omega)$ are recalled in Section 3.

2. Computing the magnetic field B .

Let us consider the problem (1.1) - (1.3). Let ω be an open subset of \mathbb{R}^3 . We set (see [23], [6])

$$(2.1) \quad \left\{ \begin{array}{l} W^1(\omega) \text{ the closure of } D(\overline{\omega}) \text{ for the semi-norm} \\ \quad \varphi \rightarrow \|\nabla \varphi\|_{L^2(\omega)} \\ W^2(\omega) \text{ the closure of } D(\overline{\omega}) \text{ for the semi-norm} \\ \quad \varphi \rightarrow \sum_{i,j} \left\| \frac{\partial^2 \varphi}{\partial x_i \partial x_j} \right\|_{L^2(\omega)}. \end{array} \right.$$

Throughout this paper, we assume that :

$$(2.2) \quad \left\{ \begin{array}{l} \overline{\omega} = \text{complement of an open set } \Omega \text{ with boundary } \Gamma = \partial \Omega = \partial \omega \\ \text{of class } C^2 \text{ and } \omega \text{ is simply connected.} \end{array} \right.$$

Then it is well known that $\varphi \rightarrow \|\nabla \varphi\|_{L^2(\omega)}$ is a norm in $W^1(\omega)$ [6]. We also introduce :

$$(2.3) \quad j_0 \in (L^2(\mathbb{R}^3))^3 \text{ with compact support and } \nabla \cdot j_0 = 0 \text{ in } \mathcal{D}'(\mathbb{R}^3).$$

Lemma 2.1. *There exists a unique solution \overline{B} of the following differential system :*

$$(2.4) \quad \left\{ \begin{array}{ll} (2.4.a) & B \in W^1(\omega)^3 \\ (2.4.b) & \nabla \wedge B = \mu_0 j_0 \quad \text{in } \omega \\ (2.4.c) & \nabla \cdot B = 0 \quad \text{in } \omega \\ (2.4.d) & B \cdot n = 0 \quad \text{on } \Gamma. \end{array} \right.$$

Moreover, if we set :

$$(2.5) \quad B_1(x) = \frac{\mu_0}{4\pi} \int_{\mathbb{R}^3} \frac{j_0(y) \wedge (x-y)}{\|x-y\|^3} dy$$

then

$$(2.6) \quad \nabla \wedge B_1 = \mu_0 j_0, \quad \nabla \cdot B_1 = 0 \quad \text{in } \mathbb{R}^3$$

$$(2.7) \quad B = B_1 + \nabla \varphi \quad \text{in } \omega$$

where φ is the unique solution of :

$$(2.8) \quad \begin{cases} (2.8.a) & \varphi \in W^2(\omega) \\ (2.8.b) & -\Delta \varphi = 0 \quad \text{in } \omega \\ (2.8.c) & \frac{\partial \varphi}{\partial n} = -B_1 \cdot n \quad \text{on } \Gamma. \end{cases}$$

Proof :

Let B_1 be defined by (2.5). Since

$$\nabla_x \left(\frac{1}{\|x-y\|} \right) = -\frac{(x-y)}{\|x-y\|^3} \quad \text{and} \quad \nabla_y \cdot j_0(y) = 0,$$

we have by differentiating (2.5)

$$(2.9) \quad \nabla \wedge B_1(x) = \frac{\mu_0}{4\pi} \int_{\mathbb{R}^3} -\nabla_x \cdot \left(\nabla_x \frac{1}{\|x-y\|} \right) \cdot j_0(y) dy = \mu_0 j_0(x)$$

$$(2.10) \quad \nabla \cdot B_1(x) = 0.$$

If $\hat{B}_1(\xi)$ denotes the Fourier transform of B_1 in \mathbb{R}^3 , as $\nabla \wedge B_1$ and $\nabla \cdot B_1$ belong to $L^2(\mathbb{R}^3)$, we have :

$$(2.11) \quad \xi \wedge \hat{B}_1(\xi) \in L^2 \quad \text{and} \quad \xi \cdot \hat{B}_1(\xi) \in L^2.$$

But :

$$(2.12) \quad \|\xi \wedge \hat{B}_1(\xi)\|^2 + (\xi \cdot \hat{B}_1(\xi))^2 = \|\xi\|^2 \|\hat{B}_1(\xi)\|^2.$$

Thus ∇B_1 belongs to L^2 which means :

$$(2.13) \quad B_1 \in (W^1(\mathbb{R}^3))^3.$$

If we set $B_2 = B - B_1$, (2.9), (2.10), (2.13) imply that problem (2.4) is equivalent to :

$$\begin{cases} (2.14.a) & B_2 \in (W^1(\omega))^3 \\ (2.14.b) & \nabla \wedge B_2 = 0 \quad \text{in } \omega \\ (2.14.c) & \nabla \cdot B_2 = 0 \quad \text{in } \omega \\ (2.14.d) & B_2 \cdot n = -B_1 \cdot n \quad \text{on } \Gamma. \end{cases}$$

Since ω is simply connected and $\partial\omega$ regular, we have (see [23], [6])

$$(2.15) \quad (B_2 \in (W^1(\omega))^3, \nabla \wedge B_2 = 0) \Leftrightarrow (B_2 = \nabla \varphi, \varphi \in W^2(\omega)).$$

Therefore (2.14) is equivalent to (2.8) where

$$(2.16) \quad B_1 \cdot n \in H^{1/2}(\Gamma), \quad \int_{\Gamma} B_1 \cdot n d\gamma = 0.$$

But the problem (2.8) has a unique solution (see [6]). This solution can be represented by a single layer representation [1], [19].

Lemma 2.2. *The solution of the problem (2.8) is given by :*

$$(2.17) \quad \varphi(x) = \frac{1}{4\pi} \int_{\Gamma} \frac{q(y)}{\|x-y\|} d\gamma(y)$$

where q is the unique solution on $H^{1/2}(\Gamma)$ of :

$$(2.18) \quad B_{1,n} = \frac{1}{2} q(x) + \frac{1}{4\pi} \int_{\Gamma} q(y) \frac{n(x) \cdot (x-y)}{\|x-y\|^3} d\gamma(y).$$

Remark 2.3. : Extension to the case where j_0 is a sum of Dirac masses : If j_0 is a compactly supported distribution on ω rather than a function f belonging to $(L^2(\mathbb{R}^3))^3$, the relation (2.5) defines a distribution over \mathbb{R}^3 belonging to $W^1(\omega \setminus \text{Supp } j_0)$. The problem (2.4), except for (2.4.a), can be solved according to (2.7) and (2.8) with $B_{1,n}$ and φ as regular as before. The local regularity of B depends on j_0 but is the same as previously (and then the same as the regularity of B_1) in a neighborhood of $\partial\omega$.

This remark is essential since numerical examples are given for distributions concentrated on wires (i.e. thin sets).

3. Variational formulation of the shape optimization problem.

We recall here classical results similar to those in [29], [30], [31], [32] (see also [25] for the two-dimensional case). We first introduce some notations.

Let ω be an open subset of \mathbb{R}^3 such that $\Omega = \overline{c\omega}$ and let V be a compactly supported vector field of class C^2 over \mathbb{R}^3 that is :

$$(3.1) \quad V \in C^2(\mathbb{R}^3, \mathbb{R}^3), V \text{ has compact support in } \mathbb{R}^3.$$

We consider transformations of Ω (or ω) given by :

$$(3.2) \quad \forall x \in \mathbb{R}^3 \quad T_t(x) = x + t V(x).$$

Then we set $\Omega_t = T_t(\Omega)$, $\omega_t = T_t(\omega)$ and we verify that $\Gamma_t = T_t(\Gamma) = \partial\Omega_t$ for t small enough (since $D_x T_t(x) = I + t DV(x)$ and thanks to the local inversion theorem).

Given $\sigma > 0$ and $G(x) \in W_{loc}^{1,1}(\mathbb{R}^3, \mathbb{R})$, with each ω_t (or Ω_t) we associate the energy :

$$(3.3) \quad E(\omega_t) = E_0(\omega_t) + \sigma P(\Omega_t) + \int_{\Omega_t} G(x) dx$$

with

$$(3.4) \quad E_0(\omega_t) = -\frac{1}{2\mu_0} \int_{\omega_t} \|B_{\omega_t}\|^2 dx$$

where B_{ω_t} is a solution of the problem (2.4) with ω_t instead of ω and $P(\Omega_t)$ is the perimeter of Ω_t . Recall that the perimeter of an open subset \mathcal{O} of \mathbb{R}^3 is defined by :

$$(3.5) \quad P(\mathcal{O}) = \sup \left\{ \langle \nabla \chi_{\mathcal{O}}, \varphi \rangle_{\mathcal{S}'(\mathbb{R}^3) \times \mathcal{S}(\mathbb{R}^3)}, \varphi \in \mathcal{S}(\mathbb{R}^3), \|\varphi\|_{\infty} \leq 1 \right\}$$

with $\chi_{\mathcal{O}}$ the characteristic function of \mathcal{O} defined by :

$$(3.6) \quad \chi_{\mathcal{O}}(x) = \begin{cases} 1 & \text{if } x \in \mathcal{O} \\ 0 & \text{otherwise} \end{cases}$$

and

$$\|\varphi\|_{\infty} = \sup_{x \in \mathbb{R}^3} \left\{ \sum_{i=1}^N \varphi_i(x)^2 \right\}^{1/2}, \quad \varphi = (\varphi_1, \dots, \varphi_N).$$

If $\partial\mathcal{O}$ is regular enough then $P(\mathcal{O})$ is the surface area of $\partial\mathcal{O}$ (see [27] and its references).

Lemma 3.1. *The functions $t \rightarrow E_o(\omega_t), P(\Omega_t), \int_{\Omega_t} G(x) dx$ are differentiable at 0 and*

we have :

$$(3.7) \quad \frac{d}{dt} \Big|_{t=0} E_o(\omega_t) = \frac{1}{2\mu_o} \int_{\Gamma} \|B\omega\|^2 (V.n) d\gamma$$

$$(3.8) \quad \frac{d}{dt} \Big|_{t=0} P(\Omega_t) = \int_{\Gamma} \mathcal{E} (V.n) d\gamma$$

where \mathcal{E} is the mean curvature of Γ .

$$(3.9) \quad \frac{d}{dt} \Big|_{t=0} \int_{\Omega_t} G(x) dx = \int_{\Omega_t} G(x) (V.n) d\gamma.$$

A sketch of the proof :

This kind of computations are classical (see for example [28], [29], [30], [21], [32] and [16] for relevant results concerning regularity of boundaries). We recall here some essential steps.

We start with the following classical formula : if g is a sufficiently regular function from $[0, \varepsilon] \times \omega$ to \mathbb{R} :

$$(3.10) \quad \frac{d}{dt} \Big|_{t=0} \int_{\omega_t} g(t,y) dy = \int_{\omega} \frac{\partial g}{\partial t} (0,y) dy - \int_{\partial\Gamma} g(y,0) (V.n) d\gamma(y)$$

(here n is always the unit normal directed towards ω). It can be obtained by an elementary change of variable $y = T_t(x)$, namely :

$$(3.11) \quad \int_{\omega_t} g(t,y) dy = \int_{\omega} g(t, y + t V(y)) \det(I + t DV(y)) dy.$$

Then by differentiation and integration by parts we obtain :

$$(3.12) \quad \frac{d}{dt} \Big|_{t=0} \int_{\omega_t} g(t,y) dy = \int_{\omega} \left(\frac{\partial g}{\partial t} (0,y) + \nabla_y g(0,y) \cdot V(y) + g(0,y) \nabla \cdot V(y) \right) dy$$

$$= \int_{\omega} \frac{\partial g}{\partial t}(0, y) dy - \int_{\Gamma} g(y, 0) (V \cdot n) d\gamma(y).$$

If we apply (3.12) to $g(t, x) = G(x)$ and Ω_t instead of ω_t we obtain (3.9). Applying (3.12) to $g(t, x) = \|B_{\omega_t}(x)\|^2$, we obtain :

$$(3.13) \quad \frac{d}{dt} \Big|_{t=0} \int_{\omega_t} \|B_{\omega_t}(x)\|^2 dx = 2 \int_{\omega} B_{\omega}(x) \cdot \frac{\partial}{\partial t} \Big|_{t=0} B_{\omega_t}(x) dx - \int_{\Gamma} \|B_{\omega}(x)\|^2 (V \cdot n) d\gamma(y)$$

By (2.7), we have :

$$(3.14) \quad B_{\omega_t} = B_1 + \nabla \varphi(t, \cdot), \quad \frac{\partial}{\partial t} \Big|_{t=0} B_{\omega_t} = \nabla_x \varphi_t(0, \cdot).$$

Then

$$\int_{\omega} B_{\omega} \cdot \frac{\partial}{\partial t} \Big|_{t=0} B_{\omega_t} dx = \int_{\omega} B_{\omega} \cdot \nabla_x \varphi_t(0, \cdot) dx = - \int_{\Gamma} (B_{\omega} \cdot n) \varphi_t d\gamma - \int_{\omega} \varphi_t \nabla \cdot B_{\omega} dx = 0,$$

the last equality coming from (2.4).

The formula (3.8) is classical (see for example [31], [32]).

Proposition 3.2. *We denote by $V(\Omega_t)$ the volume of Ω_t . Under the hypotheses (2.2), (3.1), the functions $t \rightarrow E(\omega_t)$, $V(\Omega_t)$ are differentiable at $t = 0$ and for every P constant we have :*

$$\frac{d}{dt} \Big|_{t=0} (E(\omega_t) - P V(\Omega_t)) = \int_{\Gamma} \left(\frac{1}{2\mu_0} \|B_{\omega}\|^2 + \sigma \mathcal{E} + G - P \right) (V \cdot n) d\gamma.$$

Then (B_{ω}, ω) is a solution of the equilibrium system (1.1) - (1.4) if and only if there exists P such that for every direction V satisfying (3.1) we have :

$$(3.16) \quad \frac{d}{dt} \Big|_{t=0} (E(\omega_t) - P V(\Omega_t)) = 0.$$

This immediately follows from Lemma 3.1 and Proposition 3.2. A consequence is that the solution of (1.1) - (1.4) can be considered as a critical point of the total energy $\omega \rightarrow E(\omega)$ under the constraint $V(\Omega) = V_0$ (with some regularity hypothesis).

This property is in the heart of our numerical approach.

4. Algorithm and discretization.

The algorithm consists in constructing a sequence (Γ^k, B^k, Z^k) , $k = 1, \dots, n$ where :

Γ^k is an approximation of the surface Γ at the k -th iteration of the algorithm. It is the union of triangles T_{ℓ} in \mathbb{R}^3 , $\ell = 1, \dots, L$. Each triangle is parametrized by a reference triangle of coordinates ξ and η .

The nodes of the T_{ℓ} triangles are denoted by $x^{\ell,1}, x^{\ell,2}, x^{\ell,3}$, so that if $x \in T_{\ell}$

$$(4.1) \quad x = x(\xi, \eta) = \sum_{i=1}^3 x^{\ell, i} N_i(\xi, \eta)$$

$$(4.2) \quad N_1(\xi, \eta) = 1 - \xi - \eta ; N_2(\xi, \eta) = \xi ; N_3(\xi, \eta) = \eta.$$

. If Γ^k is the boundary of the exterior domain ω_k , then B^k is an approximate solution of :

$$(4.3) \quad \begin{cases} \nabla \wedge B = \mu_0 \cdot j_0 & \text{in } \omega^k \\ \nabla \cdot B = 0 & \text{in } \omega^k \\ B \cdot n = 0 & \text{on } \Gamma^k. \end{cases}$$

. $Z^k = (\hat{Z}^{ik})_{1 \leq i \leq n}$ is the vector field which gives the direction of the displacement at each node of Γ^k . The vectors $\hat{Z}^{ik} \in \mathbb{R}^3$ are associated with the displacements $Z^{i,k}$ which are piecewise linear and related to each node ξ_i by the formula :

$$(4.4) \quad Z^{i,k}(x) = \begin{cases} \hat{Z}^{i,k} N_j(\xi, \eta) & \text{if } x \in T_\ell \text{ and } \xi^i = x^{\ell, j} \in T_\ell \\ 0 & \text{otherwise.} \end{cases}$$

At each iteration, a new surface Γ^{k+1} is constructed from Γ^k by (see [18] for a similar approach) :

$$(4.5) \quad \Gamma^{k+1}(u) = \left\{ X = x + \sum_{i=0}^n u_i Z^{i,k}(x) , u_i \in \mathbb{R} , x \in \Gamma^k \right\}.$$

Then, to update the admissible surface Γ^{k+1} we compute $u = (u_1, \dots, u_n) \in \mathbb{R}^n$. Moreover, the natural energy associated with $\Gamma^k(u)$ is :

$$(4.6) \quad E^k(u) = \frac{-1}{2\mu_0} \int_{\omega^k(u)} \|B_u\|^2 dx + \sigma \int_{\Gamma^k(u)} d\gamma + \rho g \int_{\Omega^k(u)} x_3 dx$$

where $\Omega^k(u)$, $\omega^k(u)$ are respectively the inside and the outside of $\Gamma^k(u)$ and B_u is the solution of (4.3) where $\omega^k(u)$ replaces ω^k . Here the gravity term is given by $G(x) = \rho g x_3$. In fact, B_u^k is a numerical approximation of B_u .

We take into account the constraint on the volume of $\Omega^k(u)$ by a penalty method.

Then the penalized energy is the following :

$$(4.7) \quad E_r^k(u) = E^k(u) + \frac{r}{2} (V(u) - V_0)^2$$

with $V(u)$ the volume of $\Omega^k(u)$ and V_0 given.

A critical point of this penalized energy is computed by a quasi-Newton B.F.G.S. optimization technique (see [22], [7], [8], [15], [24]). At each iteration we must compute the gradient with respect to u of the energy at $u = 0$. We denote this gradient by $DE_r^k = (D_i E_r^k)_{i=1, \dots, n}$. The derivatives $D_i E_r^k$ are given by the following lemma which is a discrete version of lemma 3.1.

Lemma 4.1. For $i=1, \dots, n$ we have :

$$(4.8) \quad D_i E_r^k = \sum_{\{l, T_\ell \ni \xi_i\}} \frac{1}{2\mu_0} \int_{T_r} \|B\|^2 (Z^{i,k,n}) \|x_\xi^\ell \wedge x_\eta^\ell\| d\xi d\eta$$

$$+ \rho g \int_{T_r} x_\xi^\ell (Z^{i,k,n}) \|x_\xi^\ell \wedge x_\eta^\ell\| d\xi d\eta + \sigma \int_{T_r} (\|x_\xi^\ell\|^2 \|x_\eta^\ell\|^2 - (x_\xi^\ell \cdot x_\eta^\ell)^2)^{-1/2}$$

$$((x_\xi^\ell \cdot Z_\xi^{i,k}) \|x_\eta^\ell\|^2 + (x_\eta^\ell \cdot Z_\eta^{i,k}) \|x_\xi^\ell\|^2 - x_\xi^\ell x_\eta^\ell (x_\eta^\ell \cdot Z_\xi^{i,k} + x_\xi^\ell \cdot Z_\eta^{i,k})) d\xi d\eta$$

$$+ r (V_k - V_0) \int_{T_r} (Z^{i,k,n}) \|x_\xi^\ell \wedge x_\eta^\ell\| d\xi d\eta$$

where T_r is the reference triangle (coordinates ξ and η), B the solution of problem (4.3), $x^\ell = x(\xi, \eta)$ an arbitrary point of T_ℓ (parametrized by (4.1)), x_ξ^ℓ, x_η^ℓ the vector derivatives of x^ℓ w.r. to ξ and η , $Z_\xi^{i,k}, Z_\eta^{i,k}$ the vector derivatives of $Z^{i,k}$ w.r. to ξ and η , V_k the volume of Ω^k (inside of Γ^k).

All these integrals are calculated exactly except the first one ; to compute this integral one must know the value of the magnetic vector field B . This imply the resolution of the exterior problem (4.3). This is the most time consuming step of the algorithm.

5. Computation of an approximation of $\|B\|^2$ over Γ^k .

The computation of the gradient DE_r^k requires the values of B^k solution of :

$$\begin{cases} \nabla \wedge B^k = \mu_0 j_0 & \text{in } \omega^k \\ \nabla \cdot B^k = 0 & \text{in } \omega^k \\ B^k \cdot n = 0 & \text{on } \Gamma^k. \end{cases}$$

We write $B^k = B_1 + B_2^k$ with B_1 given by (2.5) so that $B_2^k = B^k - B_1$ is solution of :

$$(5.1) \quad \begin{cases} \nabla \wedge B_2^k = 0 & \text{in } \omega^k \\ \nabla \cdot B_2^k = 0 & \text{in } \omega^k \\ B_2^k \cdot n = -B_1 \cdot n & \text{on } \Gamma^k. \end{cases}$$

As explained in section 2, we have $B_2^k(x) = \nabla_x \varphi^k(x)$ where φ^k is the scalar potential solution of the following Neumann exterior problem :

$$(5.2) \quad \begin{cases} \Delta \varphi^k = 0 & \text{in } \omega^k \\ \frac{\partial \varphi^k}{\partial n} = -B_1 \cdot n & \text{on } \Gamma^k \\ \varphi^k(x) = 0 \ (|x|^{-1}), \ \|\nabla_x \varphi^k(x)\| = 0 \ (\|x\|^{-2}) \text{ as } \|x\| \rightarrow \infty. \end{cases}$$

As we need to evaluate $\nabla_x \varphi^k(x)$ only on Γ^k , we choose an integral representation of the solution [6], [19], [23] :

$$(5.3) \quad \varphi^k(x) = \frac{1}{4\pi} \int_{\Gamma^k} \overline{q}(y) \frac{1}{\|x-y\|} d\gamma(y)$$

where \overline{q} is the solution of the following boundary integral equation over Γ^k (see (2.17), (2.18)) :

$$(5.4) \quad B_1(x) \cdot n = \frac{\overline{q}(x)}{2} + \frac{1}{4\pi} \int_{\Gamma^k} \overline{q}(y) \frac{n_x \cdot (x-y)}{\|x-y\|^3} d\gamma(y).$$

To solve this second kind Fredholm integral equation, we use a Galerkin method [6], [19], [23]. We introduce a basis $\{e_j^k\}_{j=1, \dots, L}$ where e_j^k is piecewise constant over Γ^k ,

that is :

$$e_j^k(x) = \begin{cases} 1 & \text{if } x \in T_j \\ 0 & \text{otherwise} \end{cases} \quad \forall j=1, \dots, L \ (L \text{ the number of triangles over } \Gamma^k).$$

Then the solution \overline{q} of (5.4) is now approximated by :

$$q^k(y) = \sum_{j=1}^L c_j^k e_j^k$$

where $(c_j^k)_{j=1, \dots, L} \in \mathbb{R}^L$ is solution of the following linear system [6], [19] :

$$(5.6) \quad (D^k + H^k) c^k = \ell^k; \quad c^k = (c_j^k)_{j=1, \dots, L}$$

$$(5.7) \quad D^k = (d_{i,j}^k)_{i,j=1}^L \quad \text{and} \quad H^k = (h_{i,j}^k)_{i,j=1}^L$$

where

$$(5.8) \quad h_{i,j}^k = \frac{1}{2\pi} \int_{T_i} \int_{T_j} \frac{n_i \cdot (x-y)}{\|x-y\|^3} d\gamma(x) d\gamma(y)$$

$$(5.9) \quad d_{i,j}^k = \begin{cases} 0 & \text{if } i \neq j \\ \int_{T_i} d\gamma(x) & \text{if } i = j \end{cases}$$

$$\ell_i^k = 2 \int_{T_i} B_1(x) \cdot n_i d\gamma(x).$$

The matrix of the system is full and not symmetric. The coefficients h_{ii}^k are equal to zero as $n_i \cdot (x-y) = 0$. Then we can compute $h_{i,j}^k$ by a Newton-Cotes method. Computation of

the coefficients ϵ_i strongly depends on $B_1(x)$. It requires numerical quadrature of the expression (2.5).

Finally, computing $\|B^k(x)\|^2 = \|B_1(x) + \nabla_x \phi^k(x)\|^2$ implies the evaluation of $\nabla_x \phi^k(x)$ which is given by :

$$(5.10) \quad \nabla_x \phi^k(x) = \frac{1}{4\pi} \int_{\Gamma^k} q^k(y) \nabla_x \left(\frac{1}{\|x-y\|} \right) d\gamma(y).$$

This is clearly a singular integral as the kernel is $\nabla_x \left(\frac{1}{\|x-y\|} \right)$ which has a singularity of order 2. As q^k is a constant on each triangle T_j , this integral is a linear combination of elementary integrals like :

$$\int_{T_j} \nabla_x \left(\frac{1}{\|x-y\|} \right) d\gamma(y)$$

which are computed at the barycenter of each triangle T_i . Only the integral where $T_j = T_i$ is singular. Integrating by parts reduces the problem to a simple integral over ∂T_j .

6. Numerical results.

We write the energy (1.5) as :

$$(6.1) \quad E(\Omega) = B_m \int_{\Omega} \|B\|^2 d\Omega + \sigma \int_{\Gamma} d\Gamma + B_g \int_{\Omega} z d\Omega$$

where the constants B_m , σ and B_g are given various values.

6.a. Some extra information on the actual computation :

We slightly modify the algorithm described in section 4 in order to improve the efficiency and reduce the computing time.

For instance, we start with a coarse grid to obtain a first rough approximation of the free surface. Once the coarse approximation is calculated, we use a refinement technique to work on a finer mesh. The displacement direction vector field Z_i associated with each node ξ_i is modified at each iteration. New directions are obtained using the normalized average of the normal vectors to the triangles in the neighbourhood of the ξ_i nodes. The linear systems are solved by a minimal residual algorithm.

The code was vectorized for a CRAY II computer. Indeed, in the boundary integral representation method, one of the most costly parts is the evaluation of the coefficients of the linear system matrix (5.6). In this section of the algorithm, we compute $h_{i,j}^k$ (see (5.8)), that is to say a double integral over each pair of triangles T_i, T_j . The vectorisation of this part of the algorithm provided a significant improvement and reduced the global time by five. The C.P.U. time for a gradient evaluation in a CRAY II computer in a case of 480 finite elements is about two seconds.

We do not have much control on the number of iterations since we do not really use any one-dimensional optimization strategy to optimize the line search in the quasi-Newton method. Indeed this would require lengthy evaluations of the magnetic field far from the free surface. We chose to allow more iterations. More analysis is now being made to improve this point.

6.b. The examples :

We now present six different examples ; in all cases we start with a sphere and a mesh of 480 finite elements.

- In Figure 1 we present two views of a bubble where the magnetic field B is created by three wires with a symmetric configuration. We do not take into account the potential energy due to the gravity as $B_g = 0$. Numerical convergence is obtained after 168 gradient evaluations (see remark above) and the final number of finite elements is 736.

- In Figure 2 the magnetic field B is created by seven wires, the configuration is also symmetric. Here we take into account the gravity since $B_g = 0,1$. Numerical convergence is obtained after 186 gradient evaluations and the number of finite elements is 576.

- In Figure 3 the magnetic field B is created by seven wires, but now the configuration is not symmetric. The free surface obtained is clearly not symmetric either. Here we take into account the gravity since $B_g = 0,1$. Numerical convergence is obtained after 208 gradient evaluations and the number of finite elements is 576.

- In Figure 4 the magnetic field B is created by the same seven wires as in the previous example but here the sense of the current has been changed in the two wires on the top. Numerical convergence is obtained after $icount = 156$ evaluations of the gradient and the number of finite elements kel is 608.

- In Figure 5 the magnetic field B is created by only one wire which turns around the liquid metal bubble. The factor of the energy due to the magnetic field B_m is 50. Numerical convergence is obtained after 248 evaluations of the gradient and with 544 finite elements.

- In Figure 6 we present the same example as before but now B_m is 100. We observe that the position of the liquid metal bubble is not the same. Convergence is obtained in 240 evaluations of the gradient and with 480 finite elements.

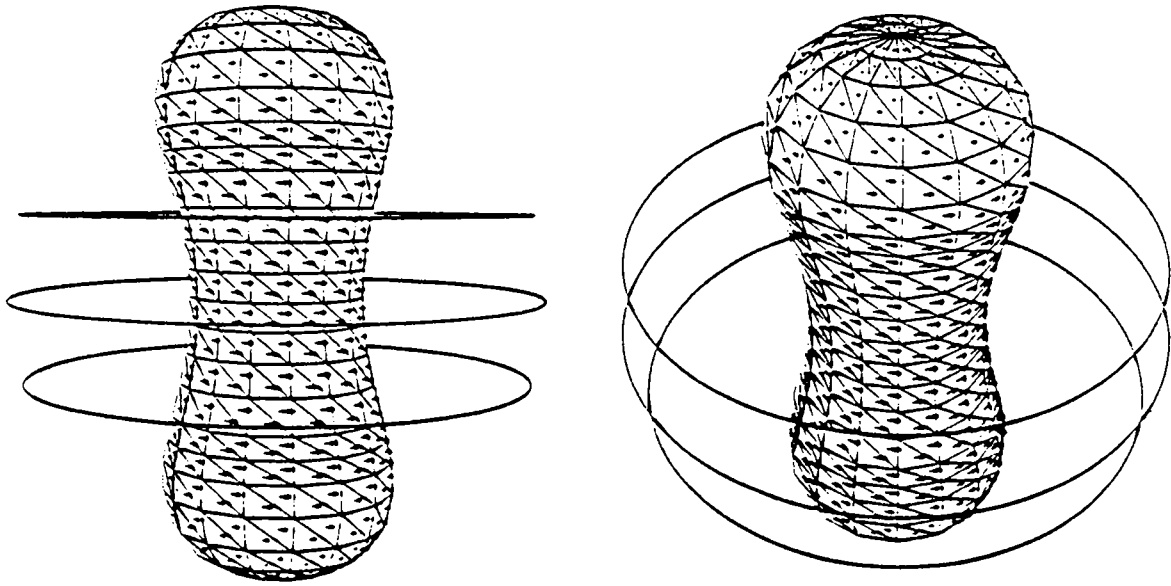


Figure 1 - $B_m = 1$; $B_g = 0$; $\sigma = 0,1$; $kel = 736$ and $icount = 168$.

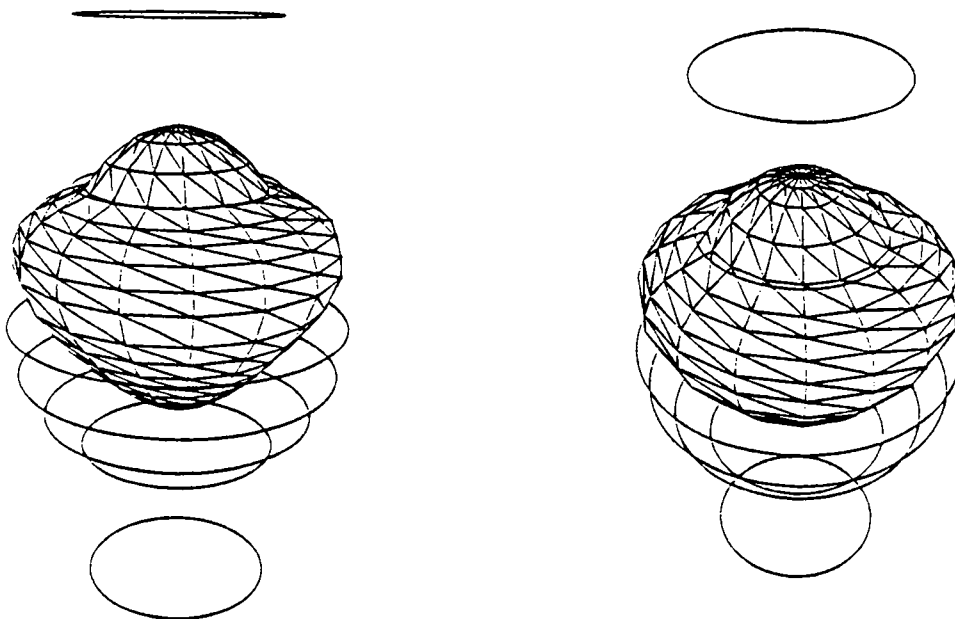


Figure 2 - $B_m = 1$; $B_g = 0,1$; $\sigma = 1$; $kel = 576$ and $icount = 186$

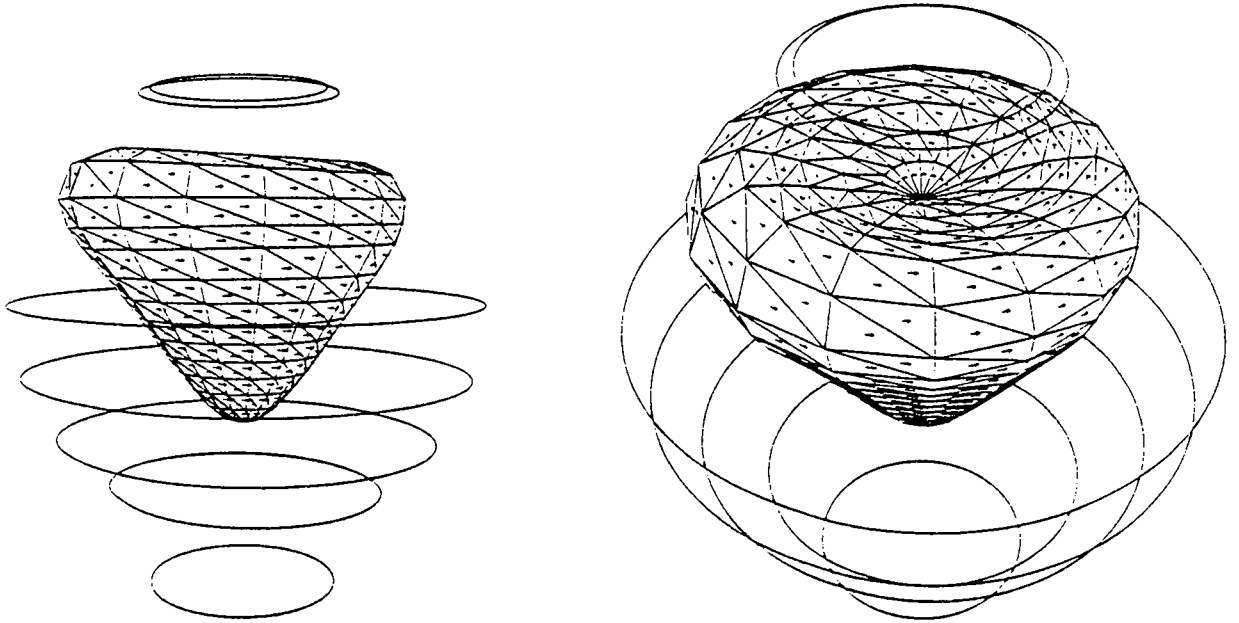


Figure 3 - $B_m = 1,0$; $B_g = 0,1$; $\sigma = 0,1$; $kel = 576$ and $icount = 208$.

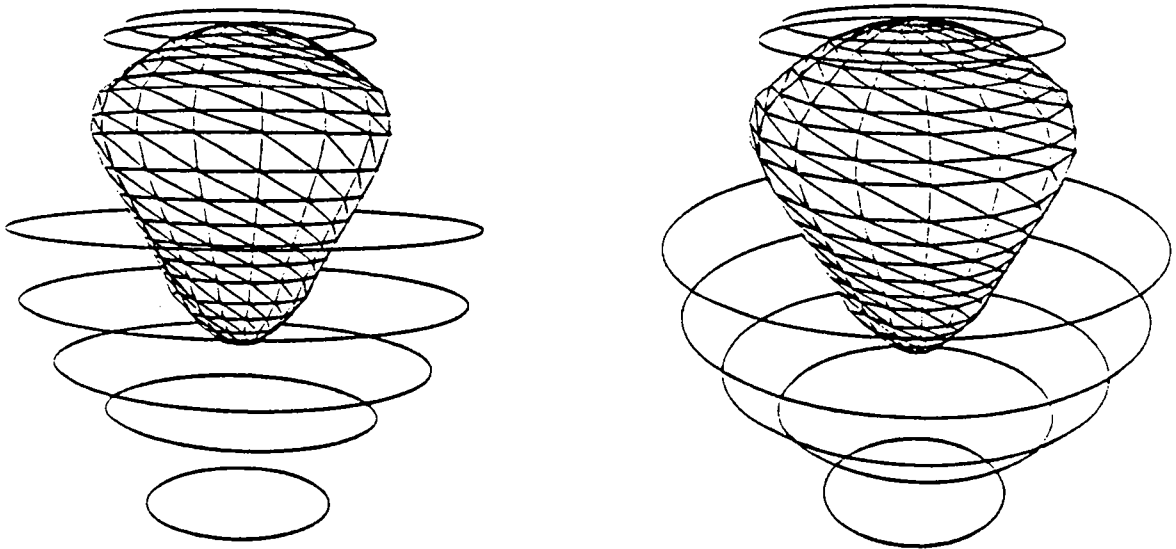


Figure 4 - $B_m = 1,0$; $B_g = 0,1$; $\sigma = 0,1$; $kel = 608$ and $icount = 156$

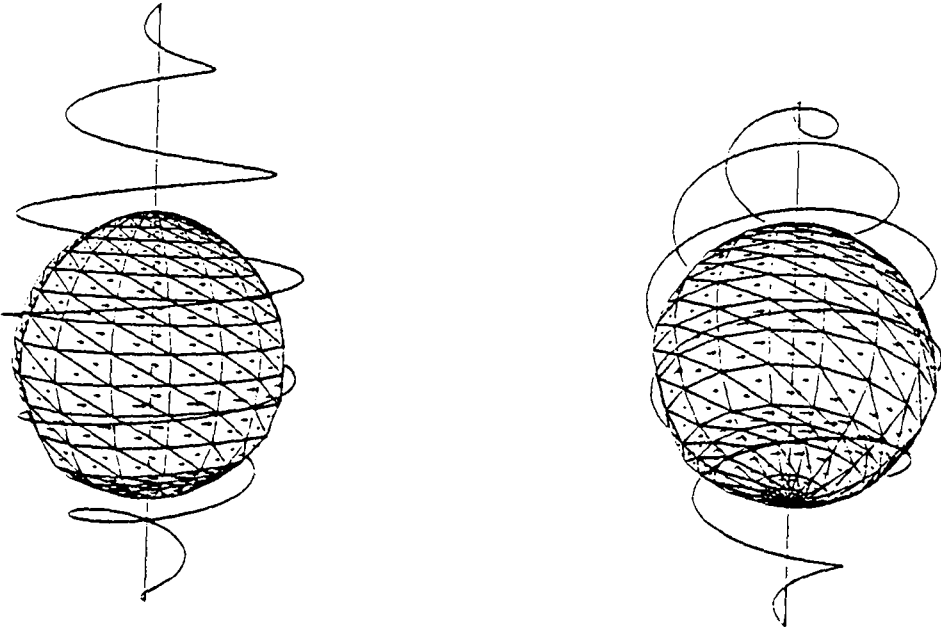


Figure 5 - $B_m = 50,0$; $B_g = 0,1$; $\sigma = 0,1$; $kel = 544$ and $icount = 248$.

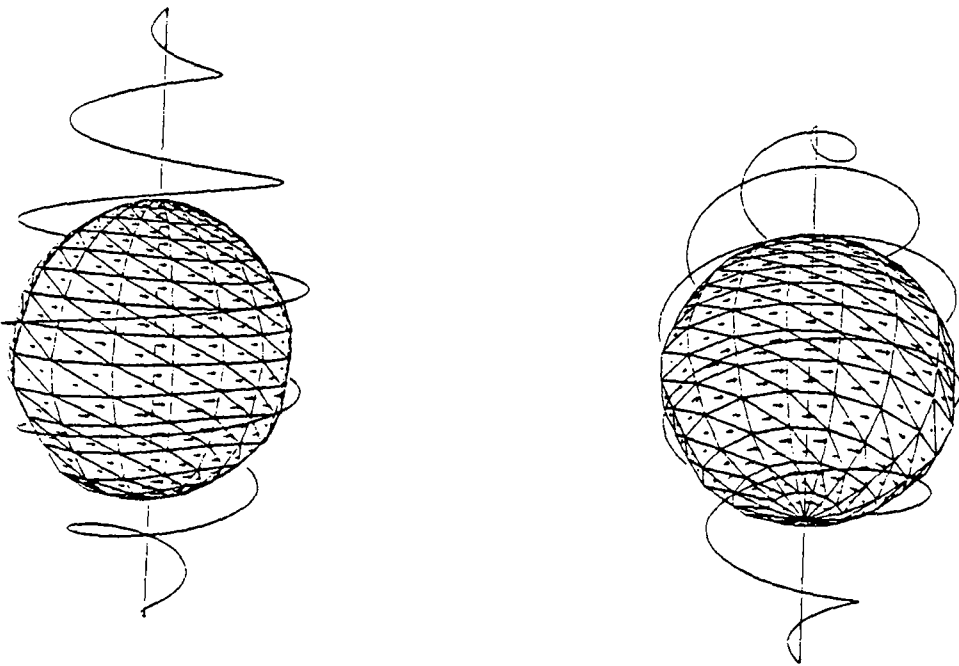


Figure 6 - $B_m = 100,0$; $B_g = 0,1$; $\sigma = 0,1$; $kel = 480$ and $icount = 240$

References

- [1] ATKINSON K.E., 1990, A survey of boundary integral equations methods for the numerical solution of Laplace's equation in three dimensions, M.A. Golberg Ed., *Mathematical concepts and methods in Science and Engineering*. Plenum Press.
- [2] BRANCHER J.-P., ETAY J., SERO-GUILLAUME O., 1983, Formage d'une lame, *J. de Mécanique Théorique et Appliquée*, 2, n°6, 976-989.
- [3] BRANCHER J.-P., SERO-GUILLAUME O., 1983, Sur l'équilibre des liquides magnétiques, applications à la magnétostatique, *J. de Mécanique Théorique et Appliquée*, 2, n°2, 265-283.
- [4] COULAUD O., HENROT A., 1991, A nonlinear boundary value problem solved by spectral methods. *Applicable Analysis*, vol. 43, 229-244.
- [5] COULAUD O., HENROT A., Numerical approximation of a free boundary problem arising in electromagnetic shaping, to appear.
- [6] DAUTRAY R., LIONS J.-L., 1988, Analyse mathématique et calcul numérique pour les Sciences et les Techniques, Vol. 5 et 6, Masson, Paris.
- [7] DENNIS J.R., J.E., MORE J.J., 1977, Quasi-Newton method motivation and theory, *SIAM REVIEW* Vol.19, N°1, 46-89.
- [8] DENNIS Jr. J.E., SCHNABEL R.B., 1983, Numerical methods for unconstrained optimization and nonlinear equations, *Prentice-Hall Series in Computational Mathematics*, 194-217.
- [9] DESCLOUX J., 1990, On the two dimensional magnetic shaping problem without surface tension, *Report n° 07.90*, Ecole Polytechnique Fédérale de Lausanne, Suisse.
- [10] ETAY J., 1982, Le formage électromagnétique des métaux liquides. Aspects expérimentaux et théoriques, *Thèse Docteur-Ingénieur*, U.S.M.G., I.N.P.G. Grenoble, France.
- [11] ETAY J., MESTEL A.J., MOFFATT H. K., 1988, Deflection of a stream of liquid metal by means of an alternating magnetic field, *J. Fluid Mech.*, 194, 309-331.
- [12] GAGNOUD A., BRANCHER J.-P., 1985, Proceedings of the Conference of Computation of Electromagnetic Fields, Fort Collins.
- [13] GAGNOUD A., ETAY J., GARNIER M., 1986, Le problème de frontière libre en lévitation électromagnétique. *J. de Mécanique Théorique et Appliquée*, 5, n°6, 911-925.
- [14] GAGNOUD A., SERO-GUILLAUME O., 1986, Le creuset froid de lévitation : modélisation électromagnétique et application. *E.D.F. Bull. Etudes et Recherches, Série B*, 1, 41-51.

- [15] GILBERT J.-Ch., LEMARECHAL C., 1988, Some numerical experiments with variable storage Quasi-Newton algorithms, *IIASA Working Paper WP-*, 88, 121, 2361, Laxenburg, Austria.
- [16] GRISVARD P., 1985, Elliptic problems in non smooth domains, *Monograph and studies in Math.*, 24, Pitman.
- [17] HENROT A., PIERRE M., 1989, Un problème inverse en formage de métaux liquides, *M² AN*, 23, 155-177.
- [18] HORNING U., MITTELMANN H.D., 1988, The augmented skeleton method for parametrized surfaces of liquid drops., *Technical Report N°113*, Arizona State University , Tempe, AZ 85287.
- [19] JOHNSON C., SCOTT L. R., 1989, An analysis of quadrature errors in second-kind boundary integral methods, *Siam J. Numer. Anal.*, Vol. 26, N° 6, 1356-1382.
- [20] LI B.Q., EVANS J.W., 1989, Computation of shapes of electromagnetically supported menisci in electromagnetic casters. Part. I : Calculations in the two dimensions. *IEEE Trans. Magnetics* , 25, N°6, 4442.
- [21] MESTEL A.J., 1982, Magnetic levitation of liquid metals, *J. of Fluid Mech.*, 117, 27-43.
- [22] MINOUX M., 1983, Programmation mathématique ; théorie et algorithmes, tome 1, Dunod, 95-126.
- [23] NEDELEC J.C., 1977, Approximation des équations intégrales en mécanique et en physique, *Rapport*, Centre de Mathématiques Appliquées, Ecole Polytechnique, Palaiseau, France.
- [24] OREN S.S., SPEDICATO E., 1976, Optimal conditioning of self-scaling variable metric algorithms, *Mathematical Programming* 10, 70-90.
- [25] PIERRE M., ROCHE J.-R., 1991, Numerical computation of free boundaries in 2-d eletromagnetic shaping, *European Journal of Mechanics, B/Fluids*, 10, N°5, 489-500.
- [26] SHERCLIFF J.A., 1981, Magnetic shaping of molten metal columns, *Proc. Royal. Soc. Lond. A* 375, 455-473.
- [27] SNEYD A.D., MOFFATT H.K., 1982, Fluid dynamical aspects of the levitation melting process, *J. of Fluid Mech.*, 117, 45-70.
- [28] SERO-GUILLAUME O., 1983, Sur l'équilibre des ferrofluides et des métaux liquides, *Thèse*, Institut Polytechnique de Lorraine, Nancy, France.
- [29] SIMON J., 1988, Second variations for domain optimization problems, Control of distributed parameter systems, *Proc. 4th Int. Conf. in Vorau*, Birkhauser Verlag.
- [30] ZOLESIO J.P., 1984, Numerical algorithm and existence result for a Bernoulli-like problem steady free boundary problem, *Large Scale Systems, Th. & Appl.* 6, n°3, 263-278.

- [31] ZOLESIO J.P., 1981, The Material derivative (or speed) method for shape optimization, in "Optimization of Distributed Parameter Structures", vol. II, J. Cea and E.J. Haud ed., Sijhoff and Nordhoff, Alphen aan den Rijn, pp 1089-1151.
- [32] ZOLESIO J.P., 1990, Introduction to shape optimisation problems and free boundary problems, *Séminaire de Mathématiques Supérieures*, Université de Montréal, Montréal, Canada.

ISSN 0249 - 6399